Exploring Self-Correlation in Flux–Gradient Relationships for Stably Stratified Conditions

P. BAAS

Royal Netherlands Meteorological Institute, De Bilt, and Meteorology and Air Quality Group, Wageningen University, Wageningen, Netherlands

G. J. STEENEVELD, B. J. H. VAN DE WIEL, AND A. A. M. HOLTSLAG

Meteorology and Air Quality Group, Wageningen University, Wageningen, Netherlands

(Manuscript received 5 December 2005, in final form 17 February 2006)

ABSTRACT

In this paper, the degree of scatter in flux–gradient relationships for stably stratified conditions is analyzed. It is generally found that scatter in the dimensionless lapse rate ϕ_h is larger than in the dimensionless shear ϕ_m when plotted versus the stability parameter z/Λ (where Λ is the local Obukhov length). Here, this phenomenon is explained to be a result of self-correlation due to the occurrence of the momentum and the heat flux on both axes, measurement uncertainties, and other possibly relevant physical processes left aside. It is shown that the ratio between relative errors in the turbulent fluxes influences the orientation of self-correlation in the flux–gradient relationships. In stable conditions, the scatter in ϕ_m is largely suppressed by self-correlation while for ϕ_h this is not the case (vice versa for unstable stratification). An alternative way of plotting is discussed for determining the slope of the linear ϕ_m function.

1. Introduction

Flux–gradient relationships are used to relate gradients of mean atmospheric profiles to turbulent fluxes. The concept of flux–gradient relationships has proven to be very useful in estimating surface fluxes both in atmospheric models and from observed profiles. The relevant quantities to relate fluxes and gradients are obtained from dimensional analysis. Consequently, the functional form of the flux–gradient relationships must be found by experiment. Some of the current problems in atmospheric boundary layer modeling (e.g., Holtslag 2006), may be associated with uncertainties in the form of the flux–gradient relationships. In the near neutral regime, different studies on the determination of the flux–gradient relationships show similar results with little scatter. In contrast, the proposed functional forms diverge considerably for stronger stability (Högström 1988, 1996; Andreas 2002).

For the stable boundary layer (SBL) a systematic difference in scatter between the dimensionless shear ϕ_m and the dimensionless lapse rate ϕ_h is found when plotted versus the stability parameter z/Λ (where Λ is the local Obukhov length). Typically, scatter in ϕ_h is larger than in ϕ_m for a large majority of field experiments (see e.g., Oncley et al. 1996; Forrer and Rotach 1997; Duynkerke 1999; Howell and Sun 1999; Yagüe et al. 2001; Cheng and Brutsaert 2005; Steeneveld et al. 2006). Figure 1 illustrates this point for observations from the Cooperative Atmosphere–Surface Exchange Study 1999 (CASES-99).

In this paper we explain the difference in scatter between ϕ_m and ϕ_h to be a result of self-correlation. Self-correlation is also referred to in literature as spurious correlation or the shared variable problem and arises when one (dimensionless) group of variables is plotted against another, and the two groups under consideration have one or more common variables (e.g., Hicks 1978; Kenney 1982; Aldrich 1995). In that case, correlation is partly caused by artificial, mathematical reasons, apart from physical and observational aspects. For plots suffering from self-correlation, the amount of scatter is not directly related to the quality of the data or the validity of the physical relationship under consideration.

Corresponding author address: Dr. P. Baas, Atmospheric Research, Royal Netherlands Meteorological Institute, Wilhelminalaan 10, P.O. Box 201, 3730 AE, De Bilt, Netherlands.
E-mail: peter.baas@knmi.nl

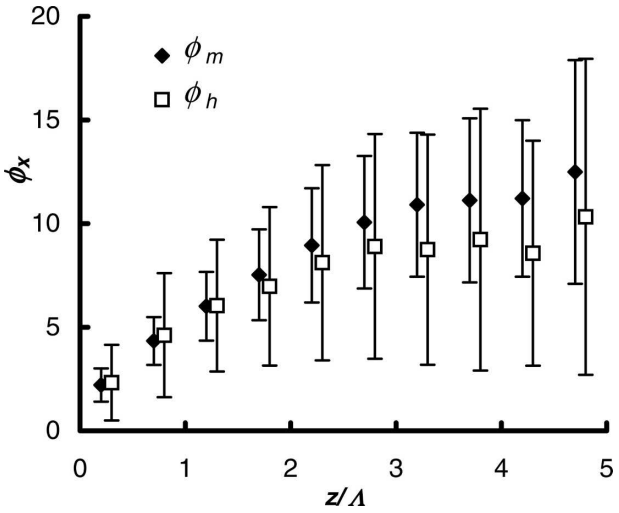

FIG. 1. Dimensionless shear (ϕ_m) and lapse rate (ϕ_h) vs stability (z/Λ) for CASES-99 observations. Error bars indicate one standard error around the mean.

In general, the influence of self-correlation depends on two factors. First, on the relative variation of the fundamental variables, $V_{x_i} = \sigma_{x_i}/\overline{x_i}$. Here σ_{x_i} denotes the standard error of a certain variable x_i. When V_{x_i} of the common variable is large compared to V_{x_i} of the other variables, the degree of self-correlation is considerable (Kim 1999; Klipp and Mahrt 2004). Second, the relationship between the orientation of the self-correlation on the one hand and of the true physical correlation on the other hand is important. Depending on this relationship, the influence of self-correlation can be either negligible or very large.

Dimensional analysis is a widely applied tool in boundary layer meteorology (e.g., Stull 1988). However, often not sufficient independent scaling variables are present to construct completely independent dimensionless groups (Andreas and Hicks 2002). As a consequence, some amount of self-correlation is often inevitable.

The aim of this paper is to explore the influence of self-correlation in ϕ_m and ϕ_h for stable conditions. Furthermore we discuss the influence of self-correlation as a function of atmospheric stability and we discuss an alternative way of plotting for determining the slope of the linear ϕ_m function independent from self-correlation. While earlier studies mainly examined the effect of the shared momentum flux, here we investigate the combined effect of the momentum flux and the heat flux on the influence of self-correlation.

In section 2 the background of Monin–Obukhov similarity theory (MOS) is briefly summarized. Section 3 gives a short description of the observational data and section 4 presents a sensitivity analysis on the influence of self-correlation on the flux–gradient relationships. In section 5 the stability dependence of self-correlation will be investigated and in section 6 we will apply an alternative technique to illustrate the influence of self-correlation. In section 7 we suggest some characteristics we think a new scaling approach should meet. Finally in section 8 we draw conclusions.

2. Monin–Obukhov similarity theory

Turbulent motions in the atmospheric surface layer can be well described in terms of MOS (e.g., Stull 1988). This theory states that under homogeneous and stationary conditions every dimensionless group is a universal function of z/L, where z is the height above the surface and

$$L = -\frac{u_*^3}{k\frac{g}{\overline{\theta}}\overline{w'\theta'_0}} \tag{1}$$

is the Obukhov length. Here k is the Von Kármán constant (taken as 0.4; Högström 1996), g is the acceleration due to gravity, and $\overline{\theta}$ is the mean potential temperature;

$$u_* = \sqrt{\tau_0/\rho} = (\overline{u'w'_0}^2 + \overline{v'w'_0}^2)^{1/4} \tag{2}$$

is the friction velocity and $\overline{w'\theta'_0}$ is the surface kinematic turbulent heat flux. The momentum flux is denoted by τ and ρ (1.2 kg m^{-3}) is the air density. Overbars indicate mean values; primes indicate deviations from the mean.

The dimensionless shear ϕ_m and the dimensionless lapse rate ϕ_h are defined as

$$\phi_m\left(\frac{z}{L}\right) = \frac{kz}{u_*}\frac{\partial\overline{U}}{\partial z} \tag{3}$$

$$\phi_h\left(\frac{z}{L}\right) = \frac{kz}{\theta_*}\frac{\partial\overline{\theta}}{\partial z} = -\frac{kzu_*}{\overline{(w'\theta')}_0}\frac{\partial\overline{\theta}}{\partial z}. \tag{4}$$

Here $\overline{U}$ is the mean wind speed and $\theta_* = -\overline{w'\theta'_0}/u_*$ is a turbulent temperature scale.

In principle MOS is only valid in the surface layer. Above this layer the magnitude of the fluxes generally decreases with height in the SBL (e.g., Stull 1988) and Monin–Obukhov scaling is no longer appropriate. Alternatively, Nieuwstadt (1984) used local fluxes instead of surface fluxes (local scaling). All dimensionless groups now depend on z/Λ, where

$$\Lambda = -\frac{u_*^3}{k\frac{g}{\overline{\theta}}\overline{w'\theta'}} \tag{5}$$

is the local Obukhov length at height z (Nieuwstadt 1984; Holtslag and Nieuwstadt 1986). MOS can be considered as a special case of local scaling theory.

3. Observational data

To illustrate our results, we use observations from the CASES-99 measurement campaign (Poulos et al. 2002), which was organized in October 1999, 50 km east of Wichita, Kansas (37.65°N, 96.74°W; ~440 m asl), over gently rolling terrain with slopes from 0.1 to 0.8 degrees. The experimental area was covered with prairie grass with a roughness length of 0.03 m.

A 60-m tower was equipped with a dense vertical array of either 20-Hz Campbell Scientific (CSAT3) or Applied Technologies K-style sonic anemometers at 10, 20, 30, 40, 50, and 55 m. Temperature profiles are obtained at six levels from slow response aspirated temperature/humidity sensors at 5, 15, 25, 35, 45, and 55 m. (All the data were obtained from http://www.atd.ucar.edu/rtf/projects/cases99/asciiDownload.jsp.)

Around the main mast a network of flux stations was set up. Hartogensis and De Bruin (2005) operated a 10 m mast with a CSAT3 sonic anemometer and a KH20 Krypton hygrometer at 2.6 and 10.2 m. To investigate the impact of self-correlation as a function of atmospheric stability, we use eddy-correlation data from the 10.2-m level. To calculate turbulent fluxes, the raw data are processed by a software package (Van Dijk and Moene 2004; see also http://www.met.wau.nl/projects/jep/report/ecromp.pdf). The package provides a statistical error for each flux variable. This error is mainly based on the measurement accuracy and the number of independent samples from which the averaged flux value is composed. For normally distributed samples the statistical error equals 2 times the standard deviation.

4. Influence of self-correlation on flux–gradient relationships

The impact of self-correlation can be investigated by imposing errors on the common variables. When the resulting contaminated points move roughly along the reference curve, self-correlation has significant influence. By reference curve we mean a first-order guess of the relationship, based on earlier studies. To be more specific, for the flux–gradient relationships in the SBL this is a log-linear relationship in the near-neutral regime. With increasing stability, the functions gradually deviate from log linear. Of course, in principle, even this first-order guess in itself suffers from self-correlation, but this second-order effect is discarded.

By imposing a 10% error on u_*, Andreas and Hicks (2002) show that self-correlation indeed causes a difference in scatter between ϕ_m and ϕ_h for unstable conditions. For stable conditions, Klipp and Mahrt (2004) found that self-correlation explains 65% of the variance between ϕ_m and z/Λ, owing to the occurrence of u_* in both quantities.

In this section we will impose errors on both the momentum flux τ and the sensible heat flux H. The erroneous fluxes can be expressed as

$$\tau_{\text{error}} = \tau_{\text{true}} + \Delta\tau$$
$$H_{\text{error}} = H_{\text{true}} + \Delta H, \tag{6}$$

where, for example, $\Delta\tau$ and ΔH can be considered as random or systematic measurement errors. In this study we ignore uncertainties in the gradients, although these can be considerable (Akima 1970; Oncley et al. 1996; Frentzen and Vogel 2001). When we reduce the errors $\Delta\tau$ and ΔH to infinitesimal values, we obtain from Eq. (6)

$$\tau_{\text{error}} = \tau_{\text{true}}\left(1 + \frac{\delta\tau}{\tau_{\text{true}}}\right)$$
$$H_{\text{error}} = H_{\text{true}}\left(1 + \frac{\delta H}{H_{\text{true}}}\right). \tag{7}$$

At first we assume the relative errors in τ and the H to be equal, so $\delta\tau/\tau = \delta H/H$. In this case, the direction in which a reference point shifts as a result of the imposed errors reads

$$\left[\frac{\partial\phi_m}{\partial(z/\Lambda)}\right]_{\text{error}} = \left[\frac{\partial\phi_h}{\partial(z/\Lambda)}\right]_{\text{error}} = \frac{\phi_m}{z/\Lambda} = \frac{\phi_h}{z/\Lambda}. \tag{8}$$

This result is found by differentiating ϕ_m, ϕ_h, and z/Λ with respect to both τ and H and using the assumption $\delta\tau/\tau = \delta H/H$ (see the appendix). Equation (8) states that the effect of an imposed error $\delta\tau/\tau = \delta H/H$ on a reference point in the ϕ, z/Λ space causes a deviation from the reference point along a line through the reference point and the origin. Equation (8) indicates that the response of ϕ_m and ϕ_h on imposed errors is exactly equal. Consequently, when $\delta\tau/\tau = \delta H/H$, any difference in observed scatter between ϕ_m and ϕ_h cannot be explained as an effect of self-correlation. For the Businger–Dyer relationships ($\phi_m = \phi_h = 1 + 5z/\Lambda$; Dyer 1974), this result implies that for increasing stability, the deviation becomes more aligned with the slope of the ϕ function, β (Fig. 2).

In reality the assumption $\delta\tau/\tau = \delta H/H$ is not generally valid (see section 5). Because often the exact correlation between $\delta\tau/\tau$ and $\delta H/H$ is unknown, we exam-

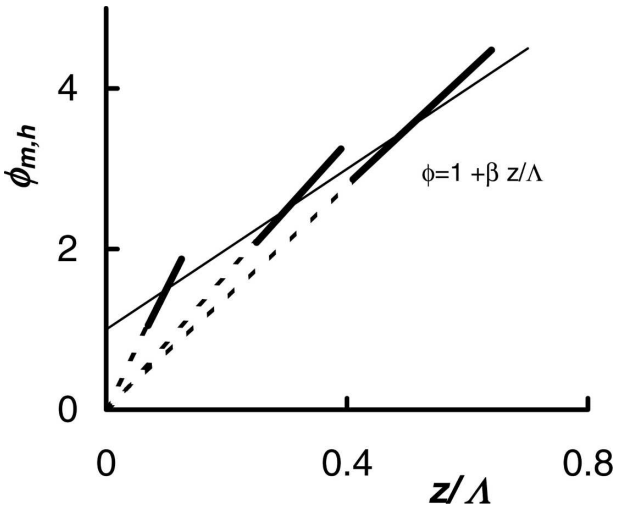

FIG. 2. Effect of errors in the momentum flux and the heat flux ($\delta H/H = \delta\tau/\tau$) on the position of a reference point in the ϕ–z/Λ space. Application to the Businger–Dyer relations ($\beta = 5$).

ine four limit situations of the error ratio parameter $\alpha = (\delta H/H)/(\delta\tau/\tau)$:

(a) $\delta\tau/\tau = \delta H/H$ ($\alpha = 1$; as above)
(b) $\delta\tau/\tau = 0$ and $|\delta H/H| > 0$ ($\alpha \rightarrow |\infty|$)
(c) $|\delta\tau/\tau| > 0$ and $\delta H/H = 0$ ($\alpha = 0$)
(d) $\delta\tau/\tau \neq \delta H/H$ ($-\infty < \alpha < \infty$)

The magnitude of the imposed relative errors is randomly taken from a uniform distribution and is between −20% and +20%. Starting from a reference point, for each of the four limit situations 100 artificial data points are generated. Figure 3 shows the results of this numerical simulation. The solid lines correspond to the reference curve, in this case the Beljaars–Holtslag (1991, hereafter BH91) formulation for momentum. The results of the current study do not depend on the choice of this specific function. Other realistic functions lead to similar conclusions.

Figure 3a confirms our analytical approach of Eq. (8): ϕ_m and ϕ_h behave similarly and all points are on a straight line through the reference point and the origin. When the relative errors in τ and the H are not equal as in the cases (b), (c), and (d), the flux–gradient functions indeed scatter differently. In these cases the random ϕ_m data scatters approximately along the reference curve, while for ϕ_h the data scatters roughly perpendicular to this curve. For case (c) this leads to the interesting paradoxical result that when τ contains an error and H is perfect, $\phi_m(z/\Lambda)$ shows little scatter while $\phi_h(z/\Lambda)$ shows large scatter. Except for Fig. 3d all points are on straight or slightly bent lines. Figure 3d shows much more scatter, because contrary to the cases (a), (b), and (c), there is no fixed correlation between $\delta\tau/\tau$ and $\delta H/H$ in this case ($-\infty < \alpha < \infty$). In fact, in case (d) the three other cases are enclosed. Figure 3 also infers that the magnitude of the deviations depends on α. For example, the maximum deviation in case (a) is much smaller than in case (d) for both ϕ_m and ϕ_h.

In general, when $\delta\tau/\tau \neq \delta H/H$, ϕ_h will always have more scatter around the reference curve than ϕ_m for a given dataset in stable conditions. This is a nonphysical effect that rises from the mathematical expressions for ϕ_m, ϕ_h and z/Λ. For ϕ_m the shift along the reference curve demonstrates that self-correlation has substantial influence, while for ϕ_h self-correlation only is important when $\delta\tau/\tau = \delta H/H$. The different behavior of ϕ_m and ϕ_h illustrates the fact that just common variables on both axes does not automatically imply that self-correlation is important. Only when the mathematical relationship of the common variables is roughly in line with the physical relationship (like in ϕ_m), scatter remains hidden and self-correlation will have significant influence.

For a given α the direction in which a certain reference point will shift due to errors in the fluxes reads for $\phi_m(z/\Lambda)$

$$\left[\frac{\partial\phi_m}{\partial(z/\Lambda)}\right]_{\text{error}} = \left(\frac{-0.5}{\alpha - 1.5}\right)\frac{\phi_m}{z/\Lambda}, \tag{9}$$

and for $\phi_h(z/\Lambda)$

$$\left[\frac{\partial\phi_h}{\partial(z/\Lambda)}\right]_{\text{error}} = \left(\frac{0.5 - \alpha}{\alpha - 1.5}\right)\frac{\phi_h}{z/\Lambda}. \tag{10}$$

These expressions are derived in the appendix and agree with the limit situations of Fig. 3. For example, when $\alpha = 1$ as in Fig. 3a, Eqs. (9) and (10) both reduce to Eq. (8). In fact, these equations predict the orientation of self-correlation for a given value of α in a certain point (z/Λ, $\phi_{m,h}$).

The above analysis can also be applied to the unstable regime. As such, it can be shown that the effect on scatter in ϕ_m and ϕ_h is then mostly opposite: in the unstable regime ϕ_m exhibits more scatter than ϕ_h (see also Andreas and Hicks 2002; Johansson et al. 2001).

5. Stability dependence of self-correlation

In section 4 we found that α influences the orientation of scatter in flux–gradient plots. In practice however, it is hard to estimate the actual value of α. In this section we show how α may be influenced by atmospheric stability.

For our analysis we use eddy-correlation data from CASES-99, but similar results were obtained with routine flux observations from the Wageningen University

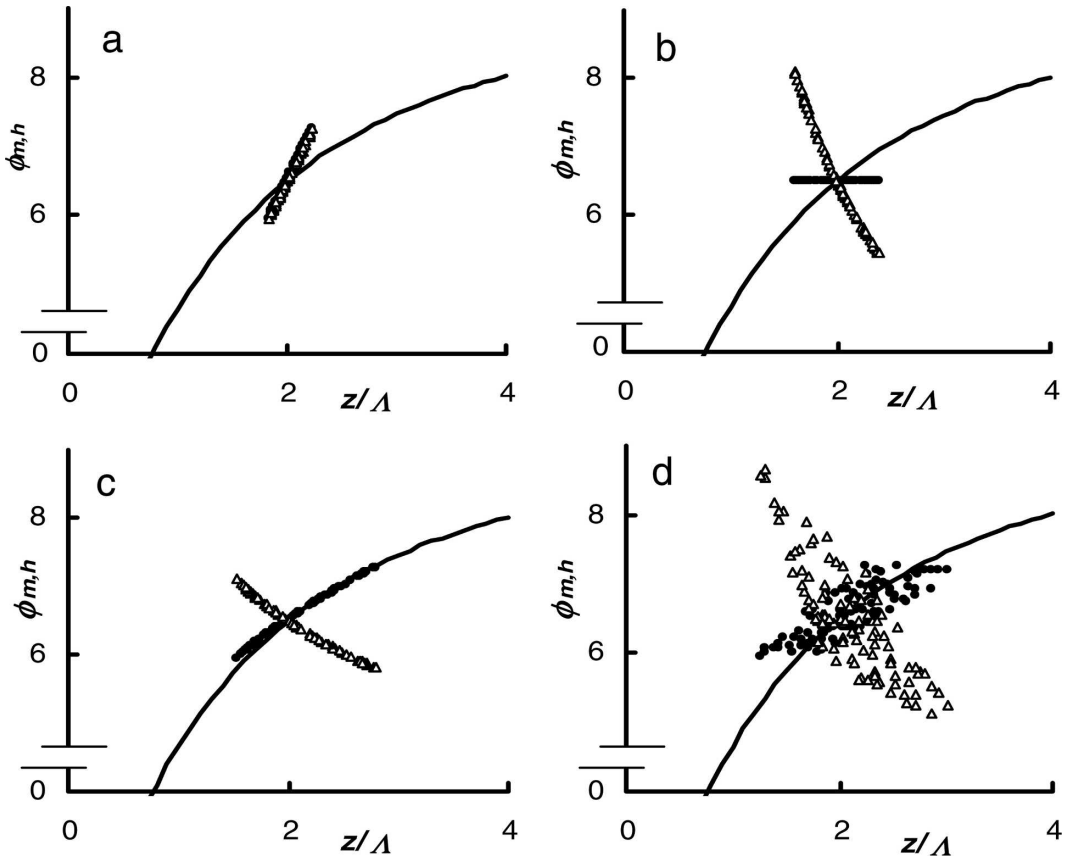

FIG. 3. The impact of errors in the momentum flux and the heat flux on plots of ϕ_h and ϕ_m vs z/Λ for different values of the ratio between $\delta H/H$ and $\delta\tau/\tau$: (a) $\delta\tau/\tau = \delta H/H$, (b) $\delta\tau/\tau = 0$ and $|\delta H/H| > 0$, (c) $|\delta\tau/\tau| > 0$ and $\delta H/H = 0$, and (d) $\delta\tau/\tau \neq \delta H/H$. Open triangles ($\Delta$) indicate ϕ_h, solid circles ($\bullet$) indicate ϕ_m. The solid line represents the BH91 function for momentum. The maximum error margin amounts to |20%|.

weather field (Jacobs et al. 2003). With the statistical error described in section 3, relative errors of τ and H can be obtained according to

$$\frac{\Delta x}{x} = \frac{\mathrm{se}(x)}{x_{\mathrm{ref}}}, \tag{11}$$

where x is τ or H and $\mathrm{se}(x)$ is the corresponding statistical error. Note that the statistical error is not equal to the actual measurement error and does also not provide information about the sign of it. Therefore, it is impossible to determine unambiguously the effect on the orientation of scatter in the flux–gradient plots. However, it is still possible to indicate that a stability dependence is present. For example, when $\mathrm{se}(\tau) \ll \mathrm{se}(H)$, it is reasonable to assume that most of the true errors in τ will also be much smaller than those in H.

We analyze α as a function of stability and anticipate which of the four cases from Fig. 3 is more likely to occur. Figure 4a shows that in the near neutral situation, the value of $\delta H/H$ is likely to be larger than the value of $\delta\tau/\tau$. This is caused by the fact that in these conditions τ has much larger values than H. In general, smaller values of a certain variable are accompanied by larger relative errors. In the weakly stable regime (Figs. 4b,c), the relative errors are slightly related, especially for small error values. To quantify the spread, we made a linear fit to the data (using perpendicular offsets) and calculated for each data point the absolute deviation from the fit. The 75th percentile of these deviations is used as an indication for the spread. In the very stable regime (Fig. 4d), this measure is increased compared to the weakly stable regime demonstrating that the relationship between the relative errors in the fluxes disappears. The difference in behavior between the stability regimes demonstrates that α depends on stability. With respect to our analysis on self-correlation this implies that, in a certain flux–gradient plot, the orientation of scatter due to errors in the turbulent fluxes also depends on z/Λ.

To summarize, the near neutral situation of Fig. 4a compares to Fig. 3b; the weakly stable situation of Figs.

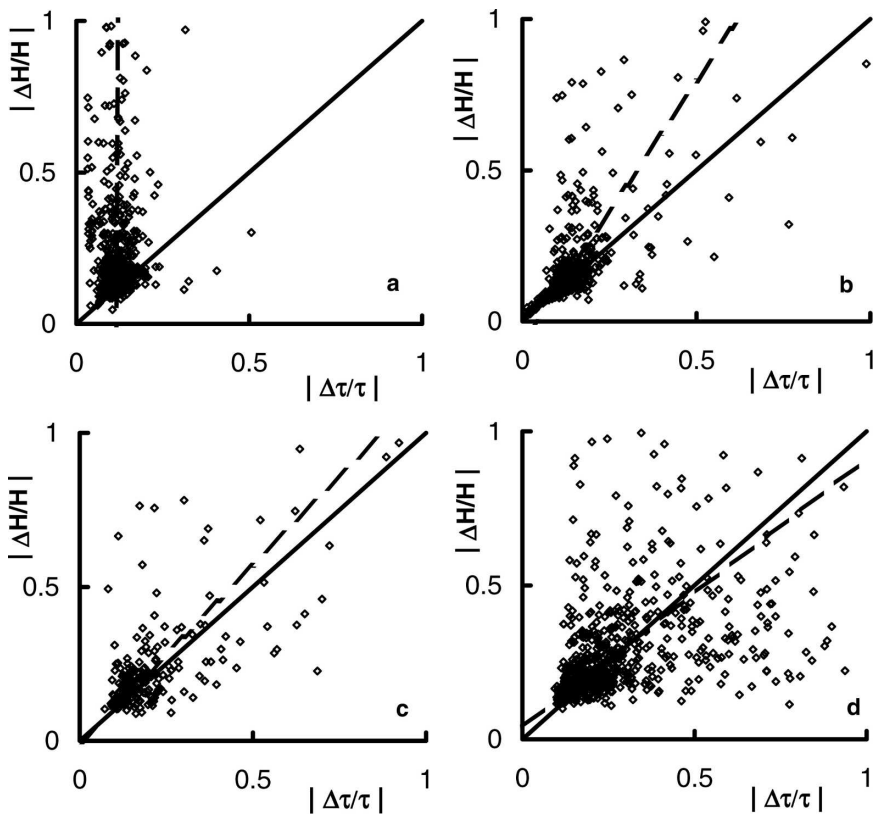

FIG. 4. Observed stability dependence of the ratio $\alpha = \delta H/H/\ \delta\tau/\tau$ for CASES-99; (a) $0 < z/\Lambda < 0.1$, (b) $0.1 < z/\Lambda < 0.5$, (c) $0.5 < z/\Lambda < 1$, (d) $z/\Lambda > 1$. The solid lines indicate the 1:1 line ($\alpha = 1$), the dashed lines indicate the least square fit based on perpendicular offsets for each stability regime. As a measure of scatter we use the 75th percentile of the deviations from the fit. The respective values are (a) 0.036, (b) 0.029, (c) 0.060, and (d) 0.109.

4b,c roughly compares to Fig. 3a; and the very stable situation of Fig. 4d compares to Fig. 3d.

6. Randomizing real observations

In this section we illustrate our earlier findings by applying an alternative method to examine self-correlation. We randomize the original dataset, by mixing all available values for each of the different variables (τ, H, dU/dz, etc.) at random. In this way the characteristic statistical distributions of the variables are conserved, which is important because only then a good comparison with the real data is possible. From the randomized data we recompute z/Λ, ϕ_m and ϕ_h. It is clear that the new data points do not have any physical meaning at all (Hicks 1981; Andreas and Hicks 2002; Klipp and Mahrt 2004; Mahrt and Vickers 2003).

Figure 5 shows the result of our analysis. For ϕ_m, the unphysical randomized points are close to the original data. This occurs because the common variable u_* appears in the denominator in both ϕ_m and z/Λ, combined with the fact that the physical relationship between ϕ_m and z/Λ has a positive slope from itself. This result corresponds to the parallel shift we found in section 4 and demonstrates again that $\phi_m(z/\Lambda)$ is heavily influenced by self-correlation.

Contrary to ϕ_m, plots of ϕ_h versus z/Λ are not affected by self-correlation in the sense that erroneous or even randomized data can still give misleadingly good results. However, the randomized data do not look completely chaotic for ϕ_h. Just as in the case of ϕ_m, the statistics of the common variables are reflected. The difference is that in ϕ_h u_* appears in the nominator, which causes the randomized ϕ_h data to show some hyperbolic relationship. This behavior corresponds to the normal shift of a reference point relative to the reference curve that we found in section 4.

The result of Fig. 5a raises the question if there is any information in a plot of ϕ_m versus z/Λ. The small differences between the randomized data and the real data cannot result from limited data ranges: Table 1 shows that for each variable the range amounts at least

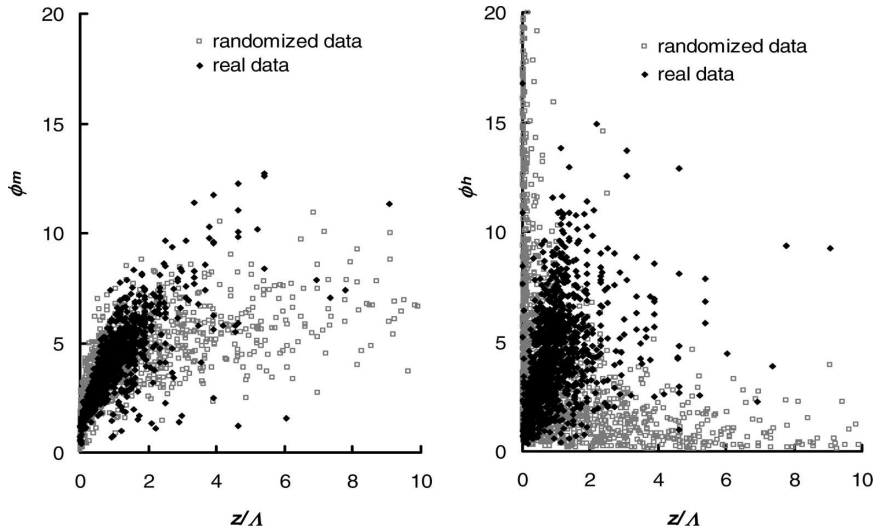

FIG. 5. Flux–gradient relationships for real and randomized data for (left) ϕ_m and (right)ϕ_h vs z/Λ. Black dots represent real data, gray squares randomized data.

a factor of 10, which is considerable. Fortunately, as is also known from practice, ϕ_m indeed contains useful information. We can determine the slope of ϕ_m versus z/Λ *independent* from self-correlation by anticipating a linear relationship of the type $\phi_m = 1 + \beta\, z/\Lambda$. Noting the definitions of ϕ_m and z/Λ and multiplying both sides with $u_*^3/(kz)$, we can plot $u_*^2 dU/dz - u_*^3/(kz)$ versus $-g/\theta\overline{w'\theta'}$ (Fig. 6b). The slope of this plot provides an independent estimate for the slope β of the standard ϕ_m plot as given in Fig. 6a. We limit our analysis to data for which $z/\Lambda < 1.5$, since only then a linear relationship can be assumed (e.g., Holtslag and De Bruin 1988; BH91). Comparing Figs. 6a and 6b shows that the slopes of both figures agree well. This indicates that, contrary to the scatter, the shape of ϕ_m is not very sensitive to self-correlation. Note that scatter in Fig. 6b is small, despite the fact that we plot a difference term on the *y* axis.

7. Discussion and future research

Scatter can be misleadingly small in plots were self-correlation is important. Consequently, there is need for an alternative way to relate fluxes and profiles. One way to deal with this problem is to search for alternative scaling approaches that are less vulnerable to self-correlation (e.g., Klipp and Mahrt 2004).

The Buckingham–Pi theorem does not prescribe how to compose the different dimensionless groups. When information on relative errors of the different variables (u_*, H, $\partial\overline{U}/\partial z$, $\partial\overline{\theta}/\partial z$, etc.) is available, it would be possible to construct the dimensionless groups in the most advantageous way. In practice this means that the most uncertain variables (here the turbulent fluxes) are raised to the lowest power in order to minimize the influence of their high relative error. Because in stable conditions fluxes are much smaller than gradients, fluxes should be raised to the lowest possible powers. In the unstable regime the situation is opposite: fluxes are large and gradients are small. Consequently, higher powers for the fluxes (e.g., u_*^3) combined with lower powers for the gradients are preferable. Based on this arguments, it can be stated that MOS is much more suitable for unstable than for stable conditions. MOS can be regarded as a flux-based scaling approach, while for the SBL a gradient-based scaling might be more suitable.

For the SBL, in many cases the above reasoning leads to a scaling based on the gradient Richardson number, which is given by

$$\mathrm{Ri} = \frac{g}{\overline{\theta}}\frac{\partial\overline{\theta}}{\partial z}\Bigg/\left(\frac{\partial\overline{U}}{\partial z}\right)^2. \tag{12}$$

By using a Ri-based scaling for the stable regime, Klipp and Mahrt (2004) also largely circumvent the problem of self-correlation (see also Sorbjan 2006).

TABLE 1. Data ranges for the relevant variables in Fig. 5.

	Min value	Max value
dU/dz (s^{-1})	0.03	0.32
$d\theta/dz$ (K m^{-1})	0.03	1.50
u_* (m s^{-1})	0.03	0.57
$\lvert\overline{w'\theta'}\rvert$ (K m s^{-1})	0.006	0.093

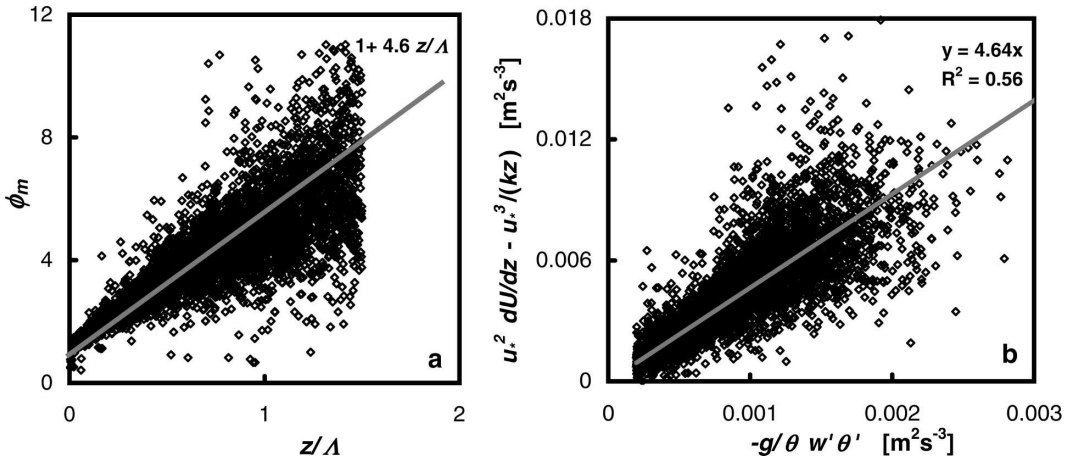

FIG. 6. (a) Standard plot of ϕ_m vs z/Λ and (b) an alternative plot from which the slope of ϕ_m vs z/Λ can be estimated independent of self-correlation. The gray line in (b) is a least square fit to the data. The slope of this fit is passed on to (a) to illustrate that this slope gives indeed a reasonable fit for the $\phi_m(z/\Lambda)$ data.

8. Conclusions

Flux–gradient relationships are traditionally used to relate turbulent fluxes and atmospheric mean profiles in the atmospheric boundary layer. However, self-correlation significantly influences the relationships between the dimensionless shear ϕ_m and the dimensionless lapse rate ϕ_h versus the stability parameter z/Λ. In general, self-correlation arises when two parameters share some common variable. For $\phi_h(z/\Lambda)$ and $\phi_m(z/\Lambda)$, the common variables are the momentum flux τ and the heat flux H. The former appears in ϕ_m, ϕ_h, and z/Λ, the latter in ϕ_h and z/Λ. Here we consider stable stratification only.

The impact of self-correlation on the flux–gradient relationships depends highly on the ratio of relative errors in the momentum flux and the heat flux. This ratio governs both the orientation and the magnitude of the scatter. In general, scatter in ϕ_m remains unrealistically small, because the data are scattered roughly along the physical curve. Contrary, for ϕ_h scatter is much larger, because the data are scattered roughly perpendicular to the physical curve; ϕ_h will therefore always show more scatter than ϕ_m. This holds only for the stable regime. In the unstable regime the effect of self-correlation is mostly reversed. In this analysis, errors associated with possible violations of Monin–Obukhov similarity theory and errors in $\partial\overline{\theta}/\partial z$ and $\partial\overline{U}/\partial z$ are not taken into account, although in reality these are also important.

When imposed relative errors on the fluxes are equal, the difference in behavior between ϕ_h and ϕ_m disappears: in both cases a reference point shifts along a straight line through this reference point and the origin. Therefore no difference in scatter between ϕ_m and ϕ_h arises in this special case. However, it is not realistic to assume the ratio between the relative errors of the fluxes to be a constant within a single dataset, because this ratio depends strongly on stability. In practice this means that in a certain flux–gradient plot, the influence of self-correlation on the orientation of the scatter also varies with stability. While self-correlation occurs in both ϕ_m and ϕ_h, only in case of ϕ_m the influence is significant. Self-correlation only becomes important when the mathematical relationship of the common variables is roughly in line with the physical relationship of the parameters that include them.

Overall, current practice of evaluating ϕ_m and ϕ_h functions from field data is troublesome. The large influence of self-correlation may lead to false confidence in the found relationship, in particular for ϕ_m. By plotting quantities in an alternative way, we are able to determine the slope of ϕ_m independent from self-correlation. It seems that, contrary to the scatter, the slope of ϕ_m is not very sensitive to self-correlation. The evaluation of ϕ_h does not suffer from artificially enhanced correlation. However, due to the factor u_*^3, small deviations in u_* may lead to large scatter, which can hamper an accurate estimation of ϕ_h.

Acknowledgments. We thank our colleagues Oscar Hartogensis and Henk de Bruin for providing their eddy-correlation data, as well as all other researchers and technicians who contributed to CASES-99. We also thank two anonymous reviewers for their constructive comments and suggestions. The first author has been supported by the Netherlands Organization for Scientific Research (NWO), in particular through the project

"land surface climate and the role of the stable boundary layer."

APPENDIX

Sensitivity of Flux–Gradient Relationships to Changes in the Momentum and the Heat Flux

The dimensionless wind shear, ϕ_m, and the dimensionless lapse rate, ϕ_h, are given by

$$\phi_m = \frac{kz}{\sqrt{\tau/\rho}}\frac{\partial \overline{U}}{\partial z} \quad \text{and} \quad \phi_h = -\frac{kz\rho c_p\sqrt{\tau/\rho}}{H}\frac{\partial \overline{\theta}}{\partial z}. \tag{A1}$$

According to Monin–Obukhov similarity theory these dimensionless groups are universal function of

$$\frac{z}{\Lambda} = \zeta = -\frac{zgk}{T}\frac{H}{\rho c_p}\left(\frac{\tau}{\rho}\right)^{-3/2}. \tag{A2}$$

We are interested in $\partial\phi_{m,h}/\partial\zeta$ as a result of imposed errors on the common variables, the momentum flux τ and the sensible heat flux H.

We assume the relative errors in the fluxes to be related:

$$\alpha\frac{\delta\tau}{\tau} = \frac{\delta H}{H}. \tag{A3}$$

First we calculate $\delta\phi_m$, $\delta\phi_h$, and $\delta\zeta$ separately, after which we perform the division. Using formal differentiation rules and Eq. (A3) we obtain

$$\delta\phi_m = kz\rho^{1/2}\frac{\partial \overline{U}}{\partial z}\delta\left(\frac{1}{\tau^{1/2}}\right) \equiv C_1\delta\left(\frac{1}{\tau^{1/2}}\right) = -\frac{1}{2}\frac{\delta\tau}{\tau^{3/2}}C_1 \tag{A4}$$

$$\delta\phi_h = -\frac{kz\rho c_p}{\rho^{1/2}}\frac{\partial \overline{\theta}}{\partial z}\delta\left(\frac{\tau^{1/2}}{H}\right) \equiv C_2\delta\left(\frac{\tau^{1/2}}{H}\right) = \frac{\frac{1}{2}H\delta\tau - \tau\delta H}{\tau^{1/2}H^2}C_2 = \frac{\left(\frac{1}{2}-\alpha\right)\delta\tau}{\tau^{1/2}H}C_2 \tag{A5}$$

$$\delta\zeta = -\frac{zgk}{T}\frac{\rho^{3/2}}{\rho c_p}\delta\left(\frac{H}{\tau^{3/2}}\right) \equiv C_3\delta\left(\frac{H}{\tau^{3/2}}\right) = \left(\frac{\delta H}{\tau^{3/2}} - \frac{3}{2}\frac{H\delta\tau}{\tau^{5/2}}\right)C_3. \tag{A6}$$

Using Eqs. (A4), (A6), and (A3) we can now calculate $\partial\phi_m/\partial\zeta$:

$$\frac{\partial\phi_m}{\partial\zeta} = \frac{-\frac{1}{2}\frac{\partial\tau}{\tau^{3/2}}C_1}{\left(\frac{dH}{\tau^{3/2}} - \frac{3}{2}\frac{H\partial\tau}{\tau^{5/2}}\right)C_3} = \frac{-\frac{1}{2}\frac{\partial\tau}{H}C_1}{\left(\frac{\partial H}{H} - \frac{3}{2}\frac{\partial\tau}{\tau}\right)C_3} = \frac{-\frac{1}{2}\frac{\partial\tau}{H}C_1}{\left(\alpha - \frac{3}{2}\right)\frac{\partial\tau}{\tau}C_3} = \frac{-\frac{1}{2}}{\left(\alpha-\frac{3}{2}\right)}\frac{\phi_m}{\zeta}. \tag{A7}$$

The same exercise can be done for $\partial\phi_h/\partial\zeta$. Using Eq. (A5), (A6), and (A3) we obtain

$$\frac{\partial\phi_h}{\partial\zeta} = \frac{\left(\frac{1}{2}-\alpha\right)\frac{\partial\tau}{\tau^{1/2}H}C_2}{\left(\frac{dH}{\tau^{3/2}} - \frac{3}{2}\frac{H\partial\tau}{\tau^{5/2}}\right)C_3} = \frac{\left(\frac{1}{2}-\alpha\right)\frac{\tau\partial\tau}{H^2}C_2}{\left(\frac{\partial H}{H} - \frac{3}{2}\frac{\partial\tau}{\tau}\right)c_3} = \frac{\left(\frac{1}{2}-\alpha\right)\frac{\tau\partial\tau}{H^2}C_2}{\left(\alpha-\frac{3}{2}\right)\frac{\partial\tau}{\tau}C_3} = \frac{\left(\frac{1}{2}-\alpha\right)}{\left(\alpha-\frac{3}{2}\right)}\frac{\phi_h}{\zeta}. \tag{A10}$$

REFERENCES

Akima, H., 1970: A new method of interpolation and smooth curve fitting based on local procedures. *J. Assoc. Comput. Mach.,* **17,** 589–602.

Aldrich, J., 1995: Correlations genuine and spurious in Pearson in Yule. *Stat. Sci.,* **10,** 364–376.

Andreas, E. L, 2002: Parameterizing scalar transfer over snow and ice: A review. *J. Hydrometeor.,* **3,** 417–432.

——, and B. B. Hicks, 2002: Comments on "Critical test of the validity of Monin–Obukhov similarity during convective conditions." *J. Atmos. Sci.,* **59,** 2605–2607.

Beljaars, A. C. M., and A. A. M. Holtslag, 1991: Flux parameterization over land surfaces for atmospheric models. *J. Appl. Meteor.,* **30,** 327–341.

Cheng, Y., and W. Brutsaert, 2005: Flux-profile relationships for wind speed and temperature in the stable atmospheric boundary layer. *Bound.-Layer Meteor.,* **114,** 519–538.

Duynkerke, P. G., 1999: Turbulence, radiation and fog in Dutch stable boundary layers. *Bound.-Layer Meteor.,* **90,** 447–477.

Dyer, A. J., 1974: A review of flux-profile relationships. *Bound.-Layer Meteor.,* **7,** 363–372.

Forrer, J., and M. W. Rotach, 1997: On the turbulence structure in the stable boundary layer over the Greenland ice sheet. *Bound.-Layer Meteor.,* **85,** 111–136.

Frentzen, P., and A. G. Vogel, 2001: Further studies of atmospheric turbulence in layers near the surface: Scaling the TKE budget above the surface layer. *Bound.-Layer Meteor.,* **99,** 173–206.

Hartogensis, O. K., and H. A. R. De Bruin, 2005: Monin–Obukhov similarity functions of the structure parameter of temperature and turbulent kinetic energy dissipation rate in the stable boundary layer. *Bound.-Layer Meteor.,* **116,** 253–276.

Hicks, B. B., 1978: Some limitations of dimensional analysis and power laws. *Bound.-Layer Meteor.,* **14,** 567–569.

——, 1981: An examination of turbulence statistics in the surface boundary layer. *Bound.-Layer Meteor.,* **21,** 389–402.

Högström, U., 1988: Non-dimensional wind and temperature profiles in the atmospheric surface layer: A re-evaluation. *Bound.-Layer Meteor.,* **42,** 55–78.

——, 1996: Review of some basic characteristics of the atmospheric surface layer. *Bound.-Layer Meteor.,* **78,** 215–246.

Holtslag, A. A. M., 2006: GEWEX atmospheric boundary layer study (GABLS) on stable boundary layers. *Bound.-Layer Meteor.,* **118,** 243–246.

——, and F. T. M. Nieuwstadt, 1986: Scaling the atmospheric boundary layer. *Bound.-Layer Meteor.,* **36,** 201–209.

——, and H. A. R. De Bruin, 1988: Applied modeling of the nighttime surface energy balance over land. *J. Appl. Meteor.,* **27,** 689–704.

Howell, J. F., and J. Sun, 1999: Surface layer fluxes in stable conditions. *Bound.-Layer Meteor.,* **90,** 495–520.

Jacobs, A. F. G., B. G. Heusinkveld, and A. A. M. Holtslag, 2003: Carbon dioxide and water vapour flux densities over a grassland area in the Netherlands. *Int. J. Climatol.,* **23,** 1663–1675.

Johansson, C., A. S. Smedman, U. Högström, J. G. Brasseur, and S. Khanna, 2001: Critical test of the validity of Monin–Obukhov similarity during convective conditions. *J. Atmos. Sci.,* **58,** 1549–1566.

Kenney, B. C., 1982: Beware of spurious self-correlations! *Water Resour. Res.,* **18,** 1041–1048.

Kim, J. H., 1999: Spurious correlation between ratios with a common divisor. *Stat. Probab. Lett.,* **44,** 383–386.

Klipp, C. L., and L. Mahrt, 2004: Flux–gradient relationship, self-correlation and intermittency in the stable boundary layer. *Quart. J. Roy. Meteor. Soc.,* **130,** 2087–2103.

Mahrt, L., and D. Vickers, 2003: Formulation of turbulent fluxes in the stable boundary layer. *J. Atmos. Sci.,* **60,** 2538–2548.

Nieuwstadt, F. T. M., 1984: The turbulent structure of the stable, nocturnal boundary layer. *J. Atmos. Sci.,* **41,** 2202–2216.

Oncley, S. P., C. A. Friehe, J. C. Larue, J. A. Businger, E. C. Itsweire, and S. S. Chang, 1996: Surface-layer fluxes, profiles, and turbulence measurements over uniform terrain under near-neutral conditions. *J. Atmos. Sci.,* **53,** 1029–1044.

Poulos, G. S., and Coauthors, 2002: CASES-99: A comprehensive investigation of the stable nocturnal boundary layer. *Bull. Amer. Meteor. Soc.,* **83,** 555–581.

Sorbjan, Z., 2006: Local structure of turbulence in stably stratified boundary layers. *J. Atmos. Sci.,* **63,** 1526–1537.

Steeneveld, G. J., B. J. H. van de Wiel, and A. A. M. Holtslag, 2006: Modeling the evolution of the atmospheric boundary layer coupled to the land surface for three contrasting nights in CASES-99. *J. Atmos. Sci.,* **63,** 920–935.

Stull, R. B., 1988: *An Introduction to Boundary Layer Meteorology*. Kluwer Academic, 666 pp.

Van Dijk, A., and A. F. Moene, 2004: The Joint Eddycovariance Project (JEP): Towards a standard for the interpretation of eddy-covariance measurements. Preprints, *16th Symp. on Boundary Layers and Turbulence,* Portland, ME, Amer. Meteor. Soc., CD-ROM, P9.1.

Yagüe, C., G. Maqueda, and J. M. Rees, 2001: Characteristics of turbulence in the lower atmosphere at Halley IV station, Antarctica. *Dyn. Atmos. Oceans,* **34,** 205–223.